Available online at www.sciencedirect.com
SCIENCE DIRECT®
Polymer 45 (2004) 2897–2909
polymer
www.elsevier.com/locate/polymer

Poly(hydroxyether sulfone) and its blends with poly(ethylene oxide): miscibility, phase behavior and hydrogen bonding interactions

Han Lü, Sixun Zheng*, Guohua Tian

College of Chemistry and Chemical Engineering, Shanghai Jiao Tong University, 800 Dongchuan Road, Shanghai 200240, China

Received 17 October 2003; received in revised form 19 February 2004; accepted 23 February 2004

Abstract

Poly(hydroxyether sulfone) (PHES) was synthesized through polycondensation of bisphenol S with epichlorohydrin. It was characterized by Fourier transform infrared spectroscopy (FTIR), nuclear magnetic resonance spectroscopy and differential scanning calorimetry (DSC). The miscibility in the blends of PHES with poly(ethylene oxide) (PEO) was established on the basis of the thermal analysis results. DSC showed that the PHES/PEO blends prepared by casting from *N*,*N*-dimethylformamide (DMF) possessed single, composition-dependent glass transition temperatures (T_gs), indicating that the blends are miscible in amorphous state. At elevated temperatures, the PHES/PEO blends underwent phase separation. The phase behavior was investigated by optical microscope and the cloud point curve was determined. A typical lower critical solution temperature behavior was observed in the moderate temperature range for this blend system. FTIR studies indicate that there are the competitive hydrogen bonding interactions upon adding PEO to the system, which was involved with the intramolecular and intermolecular hydrogen bonding interactions, i.e. –OH···O=S, –OH···–OH and –OH versus ether oxygen atoms of PEO between PHES and PEO. In terms of the infrared spectroscopic investigation, it is judged that from weak to strong the strength of the hydrogen bonding interactions is in the following order: –OH···O=S, –OH···–OH and –OH versus ether oxygen atoms of PEO.

Keywords: Poly(hydroxyether sulfone); Poly(ethylene oxide); Miscibility

1. Introduction

Polymer blending is an important alternative to obtain new polymeric materials with designed properties. A great deal amount of research work has been reported in the literature concerning miscibility, phase behavior and intermolecular interactions of polymers during the past decades [1–3]. The mixing of polymers is best described by thermodynamic, i.e. a negative free energy of mixing (ΔG_m) is necessary to achieve miscibility of polymer pairs. According to theoretical models [4–6] of polymer blends, there are three contributions to ΔG_m in high polymer blends: (1) the combinatorial entropy of mixing, (2) the 'free-volume' effect, resulting from the mismatch of the equation-of-state parameters, (3) intermolecular interactions. For high molecular weight polymers, the combinatorial entropy is negligibly small. The free-volume term is positive. Therefore, an exothermic intermolecular interaction of sufficient magnitude is a prerequisite for miscibility; in fact, most of the miscible polymer pairs found so far are caused by specific intermolecular interactions.

Poly(hydroxyether)s are a class of very important engineering thermoplastics due to their excellent mechanical properties. Among them, poly(hydroxyether of bisphenol A) (PH) has been widely applied owing to its excellent mechanical properties and dimensional stability. Due to the presence of the pendant hydroxyl groups, PH can be miscible with many proton-acceptor polymers via the intermolecular hydrogen bonding interactions and PH-containing blends could be among the most studied polymer–polymer systems [7–22]. Robeson et al. [7] first published the results of blends of PH with poly(ethylene oxide) (PEO) and the blend system was recognized to be fully miscible in the amorphous state. The miscibility was proposed to be a consequence of the potential capability of both components for intermolecular hydrogen bonding interactions, which were further confirmed with infrared spectroscopy by Coleman and Painter [14,15].

* Corresponding author. Tel.: +86-215-474-3278; fax: +86-215-474-1297.
E-mail address: szheng@sjtu.edu.cn (S. Zheng).

0032-3861/$ - see front matter © 2004 Elsevier Ltd. All rights reserved.
doi:10.1016/j.polymer.2004.02.050

The wide application of poly(hydroxyether of bisphenol A) motivates to perform structural modification to pursue the high performance. In this communication, we report the synthesis of poly(hydroxyether sulfone) (PHES), a novel polyhydroxyether. To our knowledge, there were few reports on the synthesis of PHES of high molecular weight although the condensation between bisphenol S and epichlorohydrin has widely been exploited to prepare bisphenol S type epoxy resin. From the structural point of view, PHES can be taken as a modified poly(hydroxyether of bisphenol A) (PH) owing to the introduction of sulfonyl moiety in place of isopropyl moiety in PH (see Scheme 1). Alternatively, PHES also can be taken as a modified poly(ether sulfone), another high performance thermoplastic, due to the presence of hydroxyether structural moiety.

In comparison with PH, the self-association of PHES could be more complicated, since the hydrogen bonding interactions between sulfonyl and hydroxyl group could be involved besides the self-association via hydroxyls of PHES. Due to the specific structure, PHES could form the competitive hydrogen bonding interactions when it blends with a miscible proton-acceptor polymer. For example, in the blends of PHES with PEO blends we could observe the competitive hydrogen bonding interactions among –OH···O=S, –OH···–OH and –OH versus ether oxygen atoms of PEO (i.e. intramolecular versus intermolecular) in the binary blends of PHES and PEO. Generally, the above competitive hydrogen bonding interactions are required to be formed in the ternary blends of PH, PES and PEO. There are few reports on the studies in the previous literatures.

It is of interest to compare the miscibility, phase behavior and intermolecular specific interactions of PHES/PEO blends with those of PH and PES blends with PEO due to the structural feature of PHES combining partial structural moiety of both PH and PES. In this contribution, we first present the synthesis of PHES. Thereafter, the miscibility, phase behavior and intermolecular interactions in the blends of PHES with PEO are addressed.

2. Experimental

2.1. Materials and preparation of samples

Bisphenol S and epichlorohydrin used in this work were of chemically pure grade, supplied by Beijing Chemical Reagent Co. and Yixing Chemical Reagent Co., China, respectively. PEO with a quoted average molecular weight of 20,000 was supplied by Shanghai Reagent Co., China. Poly(hydroxyether of bisphenol A) was synthesized in this lab, and it has a molecular weight of $M_n = 28,000$, measured by gel permeation chromatography (GPC), relative to polystyrene standard. The other reagents were of laboratory grades, obtained from commercial sources.

In order to synthesize 1,3-diphenoxy-2-propanol (DPP) (see Scheme 2), which acts as the model compound of hydroxyether structural unit of PHES, 45 ml of 30% aqueous NaOH (13.6703 g, 0.34 mol) was dropped to phenol (32.1252 g, 0.34 mol) and the mixture was stirred for 20 min at 50 °C. Epichlorohydrin (10.5400 g, 0.1 mol) was added and allowed to stand in these conditions for 20 min and refluxed for 3 h. The mixture was washed with chloroform three times and the organic phase was washed successively with 10 wt% aqueous NaOH and water and dried over anhydrous Na_2SO_4. The solvent was evaporated and the product was characterized by Fourier transform infrared spectroscopy (FTIR) and nuclear magnetic resonance spectroscopy (NMR).

Poly(hydroxyether sulfone) (PHES) was synthesized through direct polycondensation between bisphenol S and epichlorohydrin in the following general way. Bisphenol S (25.0270 g, 0.1 mol) was dissolved in 200 ml of dioxane and then was transferred to a 500 ml three-necked round flask equipped with a reflux condenser and a mechanical stirring bar. Epichlorohydrin (9.2531 g, 0.1 mol) was slowly added to the bisphenol S solution within 30 min with continuous stirring. Ammonium chloride (0.0161 g) was used as a catalyst and charged to the mixture. After heating the system up to 60 °C, 10 ml of 40 wt% NaOH solution was dropped to the system within 30 min. After that, the reactive system was heated up to 160 °C and refluxed for 24 h to insure complete reaction. With the reaction proceeding, the viscosity of the reacting system gradually increased and the white solids (polymer) were precipitated. The reactive system was cooled down to ambient temperature, the solid product was separated and the solution was precipitated with distilled water. The products were repeatedly washed

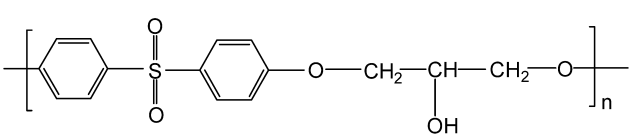

Scheme 1. Poly(hydroxyether sulfone) (PHES).

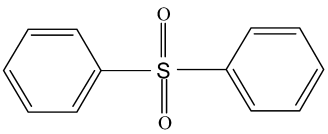

DPS

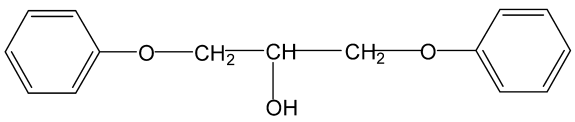

DPP

Scheme 2.

in boiling water to remove the impurity of low molecular weight. The polymer was dried in a vacuum oven before use.

The PHES/PEO blends were prepared by solution casting from *N*,*N*-dimethylformamide (DMF) at 50 °C. The total polymer concentration was 5% (w/v). To remove the residual solvent, all the blend films obtained were further desiccated in vacuo at 60 °C for 2 weeks.

2.2. Characterizations and measurement

2.2.1. Fourier transform infrared spectroscopy

FTIR measurements were conducted on a Perkin–Elmer Paragon-1000 Fourier transform spectrometer at room temperature (27 °C). Sixty-four scans at a resolution of 2 cm^{-1} were used to record the spectra. To obtain the FTIR spectra, the thin films of plain PHES and its blends with PEO were cast onto KBr windows from 2 wt % DMF solution at 60 °C. The films obtained were further dried in vacuo at 60 °C for 2 weeks to remove the residual solvent. All of the casting films used in the study were sufficiently thin to be within a range where the Beer-Lambert law is obeyed.

2.2.2. Nuclear magnetic resonance spectroscopy

NMR measurement was carried out on a Varian Mercury Plus 400 MHz NMR spectrometer at 27 °C. The polymer was dissolved with deuteronated dimethyl sulfoxide (DMSO-d_6) and the solution was measured with TMS as the internal reference.

2.2.3. Gel permeation chromatography

To measure the molecular weight of PHES, GPC measurement was performed on a Perkin–Elmer Series-2000 GPC apparatus with DMF as solvent. The molecular weights of $M_n = 36,000$ and $M_w = 64,000$ were expressed relative to polystyrene standard.

2.2.4. Differential scanning calorimetry

Thermal analysis was performed on a Perkin Elmer Pyris-1 differential scanning calorimeter in dry nitrogen atmosphere. The instrument was calibrated with a standard Indium. In order to measure glass transition temperatures, all the samples (about 10 mg in weight for amorphous samples, 5 mg for crystalline samples) were first heated up to the temperatures between glass transition and phase separation and held for 5 min to remove thermal history, followed by quenching to −70 °C. A heating rate of 20 °C/min was used at all cases. Glass transition temperature (T_g) was taken as the midpoint of the heat capacity change. The crystallization temperatures (T_c) and the melting temperatures (T_m) were taken as the temperatures of the maxima and the minima of both endothermic and exothermic peaks, respectively.

The equilibrium melting points of the PHES/PEO blends were also measured by differential scanning calorimetry (DSC). The blend samples were heated to 75 °C for 3 min to erase the thermal history, and then quenched to the desired temperature for isothermal crystallization toward completion. To measure the melting temperatures (T_ms) of the blends, the crystallized samples were heated at a heating rate of 10 °C/min and the T_ms were taken as the temperatures at which the crystals were totally molten.

2.2.5. Optical microscopy

A Leica-DMLP polarized optical microscope equipped with a hot stage (Linkam TH960, Linkam Scientific Instruments, Ltd) with a precision of ±0.1 °C was used for observation of PEO spherulites and cloud point measurement. The DMF solution of PEO and its blends with PHES were cast onto cover glasses; the major of solvent was removed at 50 °C and the residual solvent was further eliminated by drying the samples in vacuo at 50 °C for 2 weeks. The films of PEO and its blends with PHES were sandwiched between two cover glasses. For observation of spherulites, the samples were molten at 70 °C for 5 min and quenched to the desired temperature (T_c) for crystallization to completion and the spherulites were observed with the polarizing microscope in which the angle between the polarizer and analyzer was 90°. For measurements of cloud point curve (CPC), the blend films with various compositions were observed under the polarizing microscope in which the angle between the polarizer and analyzer was 45° [23]. The samples were heated through the cloud points at a rate of 5 °C/min, and the cloud point was defined as the onset of the turbidity. The cloud points were plotted as a function of blend composition.

3. Results and discussion

3.1. Synthesis and characterization of poly(hydroxyether sulfone)

In this work, the direct polycondensation of epichlorohydrin with bisphenol S was exploited to prepare poly(hydroxyether sulfone) (PHES). Figs. 1–3 show the spectra of FTIR, ^{1}H NMR and ^{13}C NMR (in DMSO-d_6) of PHES. In the FTIR spectrum, the absorption bands at 3487, 1296 and 1150 cm^{-1} were ascribed to the stretching vibrations of O–H and S=O groups, respectively, which were characteristic of the structural units of hydroxyether sulfone. Fig. 2 shows the ^{1}H NMR (in DMSO-d_6) spectrum of PHES and the proton signals were observed at $\delta = 4.1$ (m, 5H, –C*H* (OH)–, –O–CH_2– in hydroxyl ether unit), $\delta = 5.5$ (s, 1H, –O*H*), $\delta = 7.1$ (d, 4H, protons of aromatic ring), $\delta = 7.8$ ppm (d, 4H, protons of aromatic ring). The assignment of ^{13}C NMR spectrum was shown in Fig. 3. From the results of FTIR and NMR, it is seen that the poly(hydroxyether sulfone) (PHES) was synthesized by the polycondensation between bisphenol S and epichlorohydrin

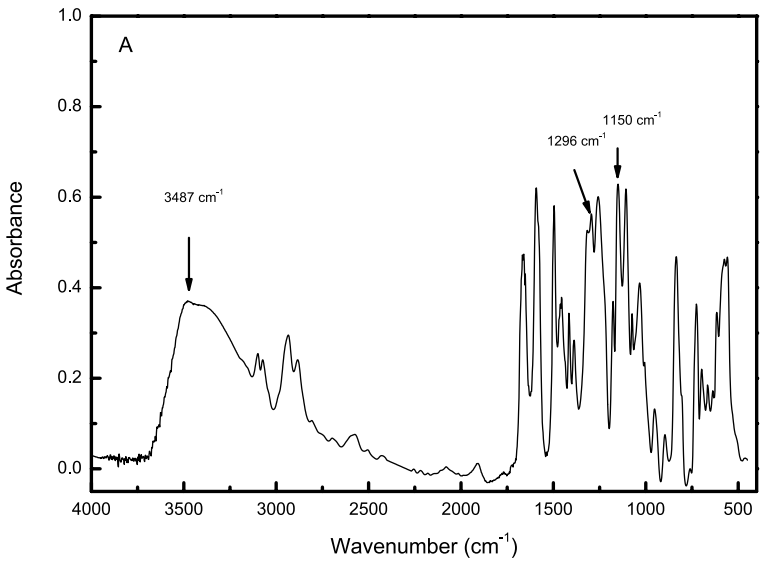

Fig. 1. FTIR spectrum of poly(hydroxyether sulfone).

in 1,4-dioxane. GPC experiment showed that the polymer with high molecular weights of $M_n = 36,000$ and $M_w = 64,000$ was obtained. The solubility of the polymer was tested using several solvents. It is interestingly noted that the structural alteration (i.e. isopropyl being replaced by sulfonyl) gives rise to a dramatic change in solubility of polymers; the PHES becomes insoluble in several common solvents of PH, such as chloroform, acetone, tetrahydrofuran (THF). The changes could be attributed to the significant changes in intramolecular interactions. The DSC result indicates that PHES is an amorphous polymer with a glass transition temperature of $T_g \approx 106$ °C, which is slightly higher than that of PH ($T_g \approx 100$ °C).

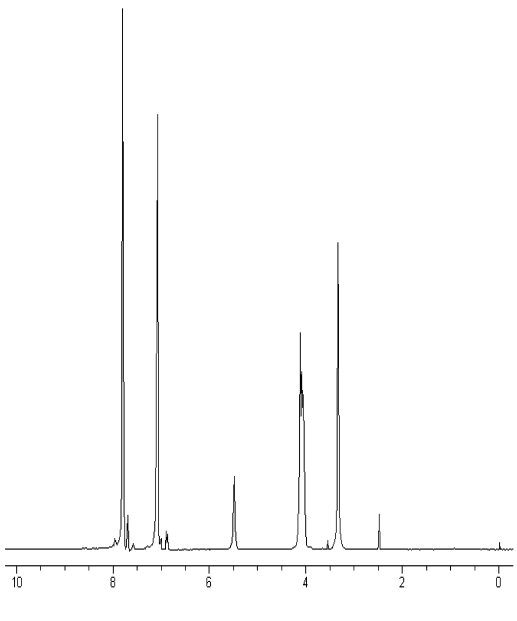

Fig. 2. ^{1}H NMR spectrum of poly(hydroxyether sulfone).

3.2. Blends of PHES with PEO

3.2.1. Miscibility and phase behavior

All the PHES/PEO blend films with PEO content lower than 40 wt% are transparent. The transparency indicates that the PHES/PEO blends present single, homogeneous, amorphous phase, i.e. no phase separation occurred at least on a scale exceeding the wavelength of visible light. It is observed that due to the formation of PEO spherulites the blends with PEO content of more than 40 wt% were not transparent; however, all the cloudy samples became transparent when heated up to 70 °C, which was above the melting point of PEO (~65 °C).

All the blend samples were subjected to thermal analysis. Fig. 4 shows the DSC curves of PHES, PEO and their blends and the thermal transitions were summarized in Fig. 5. It can be seen that each blend displayed a single glass transition temperature (T_g), intermediate between those of the two pure components and varying with the blend composition. According to the glass transition behavior, it is concluded that PHES/PEO blends are miscible in the amorphous state, i.e. possess single homogeneous, amorphous phases. Fig. 4 shows that for pure PEO, 10/90, 20/80 PHES/PEO blends, no cold crystallization transitions were observed since crystallization was sufficiently rapid and occurred to completion during the quenching. However, the DSC curves of the blends containing 70 and 60 wt% of PEO displayed cold crystallization phenomenon after glass transition and the crystallization temperatures (T_cs) increased with increase in PHES content, indicating that the crystallization of PEO becomes progressively difficult in PHES-rich blends. While the PHES content is more than 60 wt%, there is no melting transition of PEO in blends because the degree of supercooling (viz. $T_m - T_g$) is almost nonexistent, i.e. the absence of significant supercooling restricts PEO from crystallization upon cooling from the

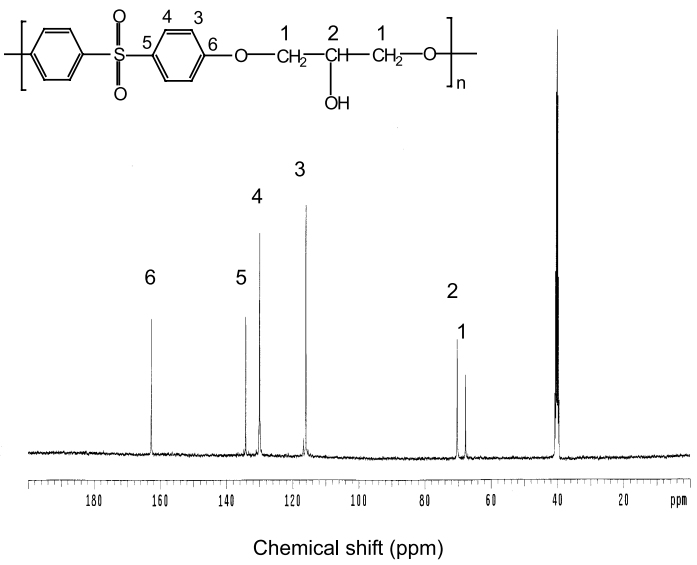

Fig. 3. ^{13}C NMR spectrum of poly(hydroxyether sulfone).

molten state, and the amorphous phase was rigid in the temperature range where PEO chains normally rearrange into the 7/2 helical conformation, which is required for crystallization to occur. In addition, the equilibrium melting temperature (T_m^0) of PEO in the blends significantly depressed with the addition of PHES to the system, suggesting a negative intermolecular interaction energy density (B_{12}) [24,25]. This is characteristic of a miscible blend composed of amorphous and crystalline polymers in which the amorphous component possesses a much higher T_g.

Fig. 6 shows the plot of crystallinity of PEO in the blends as a function of blend composition, which was calculated from the following equation [26]:

$$X_c = (\Delta H_f / w_{cryst} \Delta H_f^0) \times 100\% \quad (1)$$

where X_c is the percent crystallinity and w_{cryst}, the weight fraction of crystalline component in blends. ΔH_f is the enthalpy of fusion of crystalline component in blends and ΔH_f^0 is the fusion enthalpy of perfectly crystallized PEO, and has been reported to be 205 J/g [26]. The crystallinity of

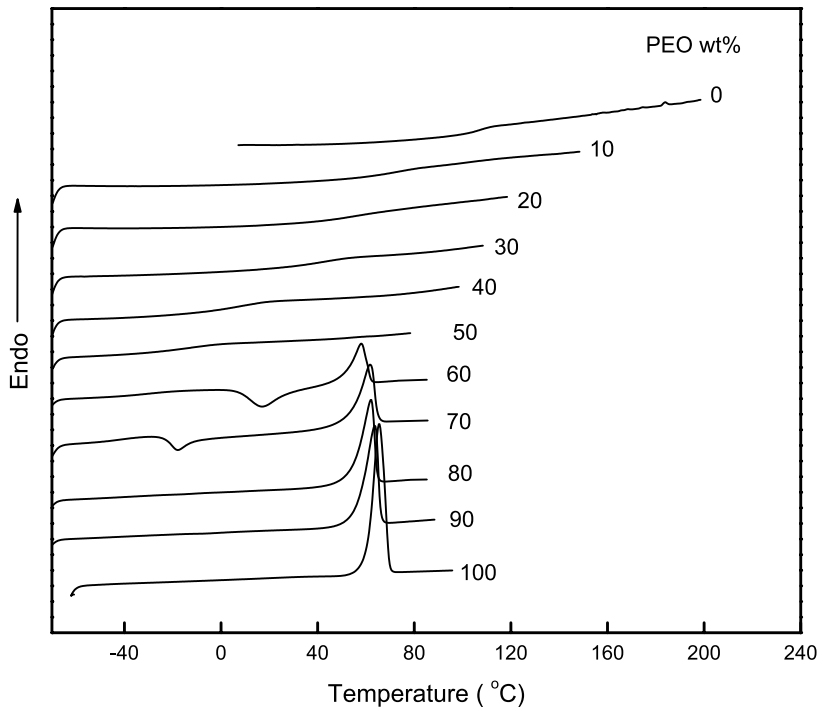

Fig. 4. DSC curves of PHES/PEO blends.

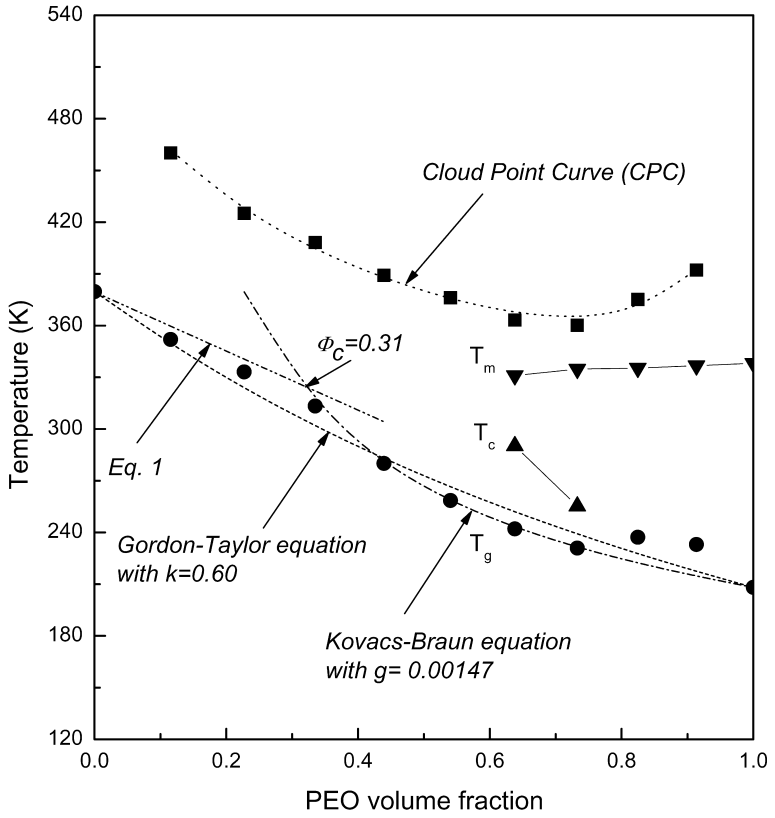

Fig. 5. Phase diagram of PHES/PEO blends: (■) cloud point curve; (▼) equilibrium melting point; (▲) crystallization temperature; (●) glass transition temperature (T_g).

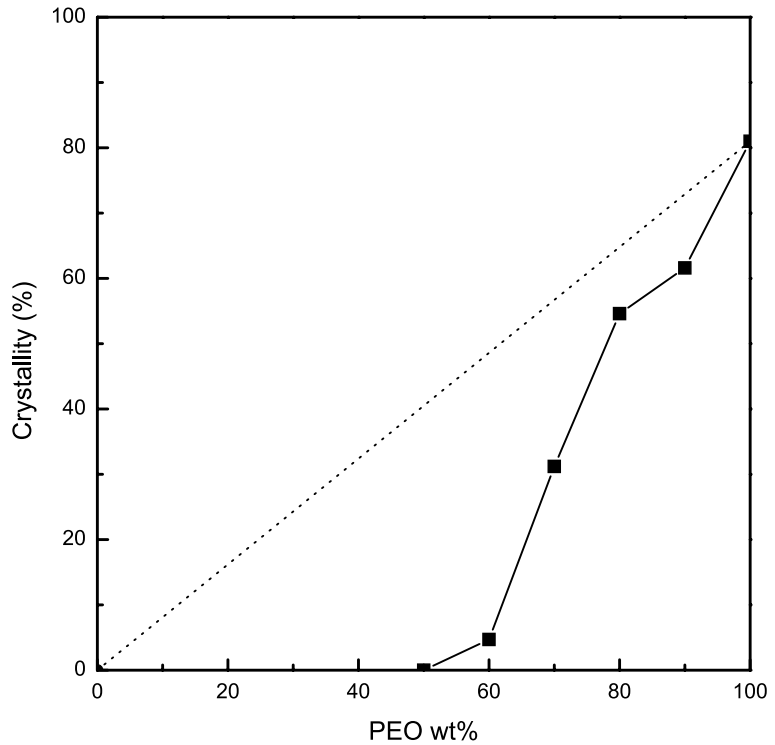

Fig. 6. Percent crystallinity of PEO in PHES/PEO blends: (■) the second DSC traces; dashed line represents the crystallinity of PEO in blends if the crystallization process was not influenced by the presence of PHES.

PEO in the blends containing PHES dramatically deviates from the dashed line, which stands for the crystallinity of PEO in the blends if the crystallization process were not influenced by the presence of PHES, suggesting a pronounced inhibition of crystallization by the presence of PHES. The supercooling of PEO crystallization decreased with increasing PHES contents in the miscible blends. The absence of significant supercooling will restrict PEO from crystallization upon cooling from the molten state; the amorphous phase is vitrified and thus crystallinity decreases dramatically with increasing PHES contents.

There are several theoretical and empirical equations to describe the dependence of glass transition temperature on blend composition. Among them the additivity, Fox [27] and the Gordon–Taylor [28] equations are mostly used. The additivity equation is shown below

$$T_g = W_1 T_{g1} + W_2 T_{g2} \tag{2}$$

where W_i is the weight fraction of component i and T_g, the glass transition temperature of blend, assuming that the specific heats of the two components are identical. For the present system, Fox equation failed to fit the experimental T_g values in the entire composition. The Gordon–Taylor equation [28] was also applied to account for T_g–composition relationship of the system:

$$T_g = \frac{W_1 T_{g1} + k W_2 T_{g2}}{W_1 + k W_2} \tag{3}$$

where $k = \Delta\alpha_{p2}/\Delta\alpha_{p1}$, and $\Delta\alpha_{pi}$ is the difference in the thermal expansion coefficient between the liquid and glassy state at T_{gi}. The equation can describe the effects of thermal expansion on the T_g. In general, the k is an adjusting parameter related to the degree of curvature of the T_g–composition curve. Prud'homme et al. [29,30] proposed that in miscible polymer blends, the quantity k can be taken as a semi-quantitative measure of strength of the intermolecular interaction between components of polymer blends. The Gordon–Taylor fit to the data yielded a k value of 0.60 and, however, failed to reproduce the T_g–composition variation (see Fig. 5).

These classical equations predict that T_g increase continuously (smoothly) and monotonically with blend composition. However, it was observed that the T_g–composition variation of several polymer blend systems is not monotonic and exhibits a cusp (or break) at the certain critical composition [31–33]. This phenomenon becomes very prominent when the T_g difference between the two homopolymers exceeds 50 °C. The classical equations become invalid below a critical temperature, $T_{crit.}$, since the free volume of the high T_g component becomes zero. Kovacs [34] has proposed that the critical temperature, $T_{crit.}$, and the critical composition, $\phi_{crit.}$, are given by:

$$T_{crit.} = T_{g2} - (f_{g2}/\Delta\alpha_2) \qquad \text{if } T_{g2} > T_{g1} \tag{4}$$

$$\phi_{crit.} = \frac{f_{g2}}{\Delta\alpha_1 (T_{g2} - T_{g1}) + f_{g2}(1 - \Delta\alpha_1/\Delta\alpha_2)} \tag{5}$$

where $\Delta\alpha_2$ is the difference between the volume expansion coefficients in the glass and liquid states of component 2 and f_{g2} is the free volume fraction of polymer 2 at T_{g2}. Below $T_{crit.}$, the T_g of blend is described by:

$$T_g = T_{g1} + \left(\frac{f_{g2}}{\Delta\alpha_1}\right)\left(\frac{\Phi_2}{\Phi_1}\right) \tag{6}$$

According to this equation, the blend T_g is uniquely determined by the properties of lower T_g component at temperature below $T_{crit.}$ or at composition below $\phi_{crit.}$. If there is excess volume between the two polymers upon mixing, Braun and Kovacs [35] have derived the following equations:

$$T_g = T_{g1} + \frac{\Phi_2 f_{g2} + g\Phi_1\Phi_2}{\Phi_1 \Delta\alpha_1} \tag{7}$$

where g is an interaction term defined as:

$$g = \frac{(V_e/V)}{\Phi_1 \Phi_2} \tag{8}$$

where V_e is the excess volume and V, the volume of the blend. The excess volume (or g) is positive if blend interactions are stronger than the average interactions between molecules of the same species, and it is negative otherwise. Effectively, g is obtained by fitting the T_g–composition data to the Braun–Kovacs equation.

For the present blend system, the composition of the blends was expressed in terms of volume fraction (see Fig. 5). In the calculation, the density values of 1.13 g/cm^3 for amorphous PEO [36] and 1.26 g/cm^3 for PHES were used, which was estimated by group contribution method [36]. The above three different equations were applied to account for the T_g–composition relationship. On the basis of the classical values of $f_{g2} = 0.025$ and $\Delta\alpha_2 = 0.00048$ K^{-1}, the critical temperature and volume fraction (with respect of PHES) are obtained to be 440 K and 0.73, respectively. Fig. 5 shows that Fox and Braun–Kovacs equations can well account for the T_g–composition dependence above and below $\phi_{crit.}$, respectively. The Braun–Kovacs fit yielded a g value of 0.00146. The positive value suggests that the blend interactions are stronger than the average interactions between molecules of the same species, which is in a good agreement with the results of the infrared spectroscopy (see infra). It is seen that the crossover from the classical (Fox) limit to the free volume (Kovacs) regime occurred at about 0.31, which is satisfactorily close to the value of 0.29 predicted by Braun–Kovacs equation. It should be pointed out that at the high content of PEO (e.g. PHES/PEO 20/80, 10/90 (wt)), the T_g of the blend positively deviates from the predicted, which is due to the enrichment of the high-T_g PHES induced by crystallization of PEO and the reinforcement of PEO spherulites of amorphous region [22,37–41].

At elevated temperatures, the PHES/PEO blends

underwent phase separation. The initially clear films became opaque upon heating beyond a certain temperature for each blend, and became clear again when the sample was cooled, i.e. the process is reversible. Such reversibility was a typical signature of lower critical solution temperature (LCST) behavior. In this work, the phase behavior was investigated by optical microscope and the CPC was determined. Fig. 7 shows an optical micrograph of PHES/PEO 90/10 blend when heated up to 200 °C. This lower consolute type of phase behavior further substantiates the miscibility at temperature below the cloud point and suggests that the two polymers are miscible as a result of an exothermic interaction (e.g. hydrogen bonding). A highly interconnected two-phase morphology with uniform domain size is some of the familiar characteristics of spinodal decomposition [42]. The asymmetrical phase diagram has the minimum around 30 wt% PEO and the system exhibits a typical LCST behavior at ca. 90 °C (see Fig. 5). It is interesting to note that the phase behavior of blends is comparable with that in the blends of poly(ether sulfone) (PES) and PEO as shown by several groups [43–46]. It is plausible to think that in the blends, the increase in temperature decreases the favorable intermolecular interaction, which in turn results in phase separation.

3.2.2. Equilibrium melting point depression

Analysis of equilibrium melting point for semi-crystalline polymer and amorphous polymer blends can give the information about miscibility and polymer–polymer interactions. Equilibrium thermodynamics predicts that by addition of a miscible diluent the chemical potential of the crystalline polymer will be decreased, which will result in the depression of equilibrium melting points. In the miscible polymer blends, the melting points could be depressed due to thermodynamic and/or morphological reasons. To eliminate the morphological effect, the melting point of PEO and its blends with PHES were analyzed by Hoffman–Weeks method [47]. The plots of the experimental melting temperatures (T'_m) as a function of crystallization temperature (T_c) are shown in Fig. 8. It can be seen that in the range of the crystallization temperatures investigated, the T'_m increased linearly with the T_c. The experimental data can be fitted by the Hoffman–Weeks equation [47,48]

$$T_m = \Phi T_c + (1 - \Phi)T_m^0 \tag{9}$$

where T_m^0 is the equilibrium melting point; $\Phi = 1/\gamma$, the stability parameter which depends on the crystal thickness, whereas γ is the ratio of the lamellar thickness l to the lamellar thickness of the critical nucleus l^* at T_c. In Eq. (9), Φ may assume the values between 0 and 1, $\Phi = 0$ implies $T_m = T_m^0$, whereas $\Phi = 1$ implies $T_m = T_c$. Consequently, the crystals are most stable for $\Phi = 0$ and inherently unstable for $\Phi = 1$. As shown in Fig. 8, the values of T_m^0 can be evaluated by extrapolating the least-squares fit lines of the experimental data according to Eq. (9) to intersect the line of $T_m = T_m^0$. The Φ parameters can be determined from the slope of these fit lines. Both, the values of T_m^0 and of Φ for the blend composition investigated are summarized in Table 1. The values of the stability parameters Φ range from 0.167 to 0.262, suggesting that the crystals are quite stable. The data of equilibrium melting points obtained in the study were further analyzed with the Nishi–Wang equation [24,25], which is based on the Flory–Huggins theory. The T_m depression is derived as follows:

$$\frac{1}{T_m^{0\prime}} - \frac{1}{T_m^0} = -\frac{BV_{2u}}{\Delta H_{2u} V_{1u}}\left(\frac{\phi_2^2}{T_m^{0\prime}}\right) \tag{10}$$

where the subscripts 1 and 2 denote the amorphous and crystalline components, respectively. ϕ_2 is the volume fraction, V_u, the molar volume of the repeating unit, ΔH_{2u} refers to the fusion enthalpy per mole of 100% crystalline PEO, $T_m^{0\prime}$ and T_m^0, the equilibrium melting points of the blends and the pure crystalline component, R, the universal gas constant, B is the interaction energy density. The interaction parameter χ_{12} can be written as:

$$\chi_{12} = \frac{BV_{1u}}{RT} \tag{11}$$

In this work, several constants were taken as $\Delta H_{2u} = 205$ J/g [26] and $V_{1u} = 212.23$ cm^3/mol and $V_{2u} = 38.9$ cm^3/mol,

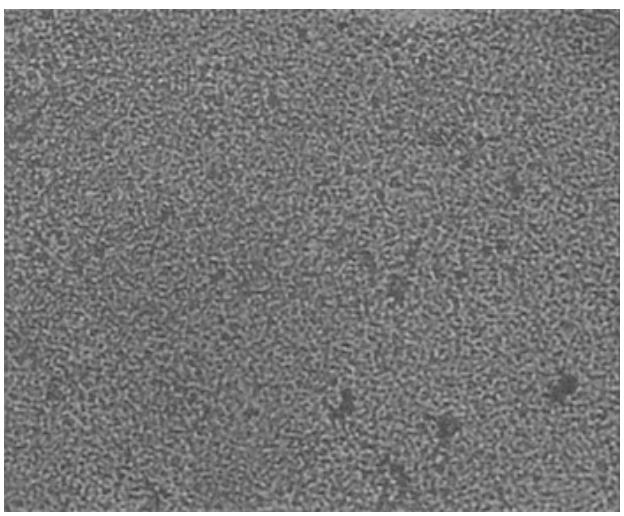

Fig. 7. Optical micrograph of the phase-separated structure for the 90/10 PHES/PEO blend taken in a hot-stage microscope at 200 °C (the original magnification was 100 × and the micrograph has been reduced to 50% of its original size for publication).

Table 1
Values of equilibrium melting points, the stability parameters and glass transition temperature, T_g for PHES/PEO blends

PHES/PEO (wt)	T_m^0 (°C)	Φ	T_g (°C)
0/100	69.3	0.161	−65.0
10/90	68.1	0.172	−40.1
20/80	67.3	0.194	−35.9
30/70	66.2	0.214	−42.2
40/60	65.1	0.262	−31.1

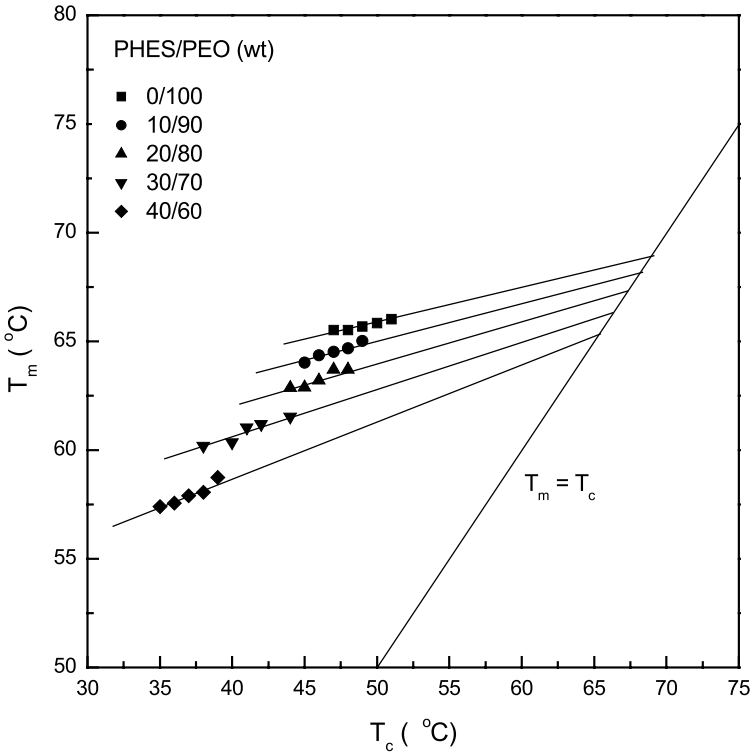

Fig. 8. Hoffman–Weeks plot for determination of equilibrium melting point (T_m^0) for PHES/PEO blends.

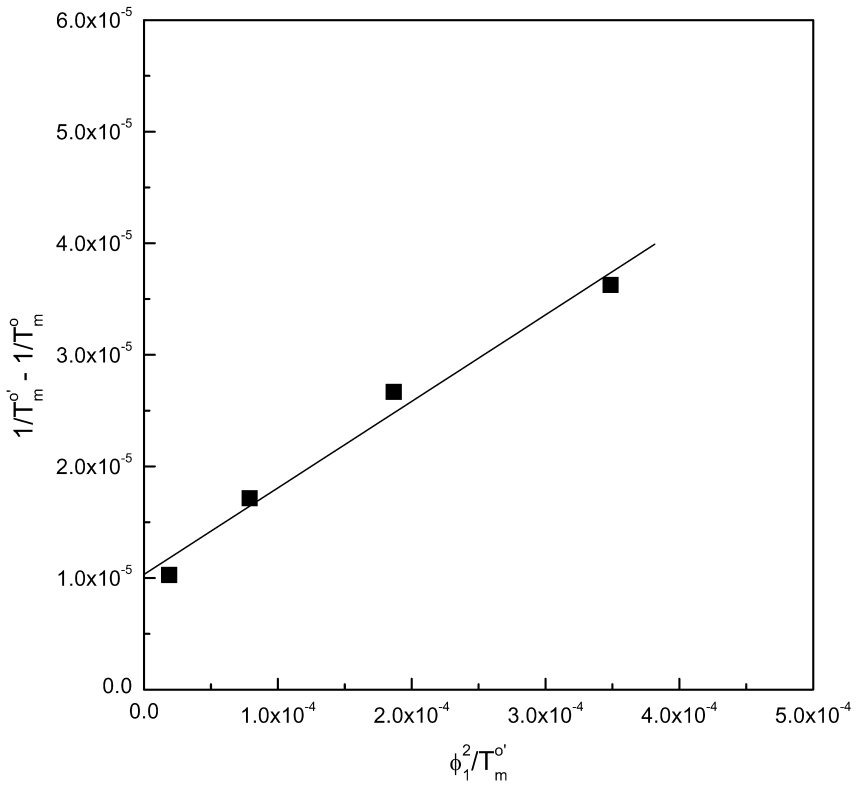

Fig. 9. Determination of intermolecular interaction parameters, B and χ_{12} for PHES/PEO blends.

which were estimated by group contribution method [36]. Assuming that B (or χ) is composition-independent, a plot of the left terms of Eq. (10) versus $\phi_1^2/T_m^{0'}$ should yield a straight line with a slope proportional to B and zero y-intercept. Fig. 9 shows the plot and the linearity of the experimental data is quite good. It is noted that the plot yielded a positive intercept. The presence of the positive intercept might be the result of a residual entropic effect [24,25,49,50], which may be due to the molecular weight of PEO [51]. From the slope, B and consequently χ_{12} were obtained to be -0.47 cal/cm^3 and -0.15 at 345 K, and the negative value of B (or χ_{12}) suggests that the PHES/PEO blends are miscible in the melt state. It is noted that the absolute value (0.15) of the χ_{12} is much smaller than the value of 0.94 obtained by Iruin et al. [52] and the value of 0.74 by Jungickel et al. [16] for the blends of PH and PEO. The decreased polymer interaction parameter (absolute value) indicates that the intermolecular interactions were weakened. The reduction could be ascribed to the structural alteration of PHES in comparison with PH, i.e. the replacement of isopropyl by sulfonyl groups gives rise to the reduction of intermolecular hydrogen bonding interactions due to the formation of the intramolecular hydrogen bonding interactions.

3.2.3. Hydrogen bonding interactions

Intramolecular specific interactions of PHES. PHES is a self-associated polymer due to the presence of the secondary hydroxyl group and sulfonyl moiety in the macromolecular backbone. The intramolecular interactions could be involved with the self-association of hydroxyls (–OH···–OH) and hydroxyl versus sulfonyl hydrogen bonding (–OH···O=S). In order to compare the relative strength of the two kinds of hydrogen bonding interactions, we investigated the FTIR spectra of poly(hydroxyether of bisphenol A) (PH) and PHES. Fig. 10 shows the FTIR spectra of PHES and PH in the frequency range of 3100–3800 cm^{-1}, the spectroscopic bands are ascribed to hydroxyl stretching vibration. The very broad bands reflect the wide distribution of hydrogen-bonded hydroxyl stretching frequencies. The shoulder bands centered at 3570 cm^{-1} are ascribed to the free hydroxyls [15]. The frequency difference ($\Delta\nu$) between the free H-bonded hydroxyl stretching vibration is a measure of the average strength of the intermolecular and/or intramolecular interactions [53,54]. We assigned the value of $\Delta\nu = 83$ cm^{-1} to the hydroxyls which was H-bonded with sulfonyl group (i.e. at 3487 cm^{-1}), whereas the value of $\Delta\nu = 221$ cm^{-1} to the hydroxyls via –OH···–OH association. To confirm this assignment, we measured the

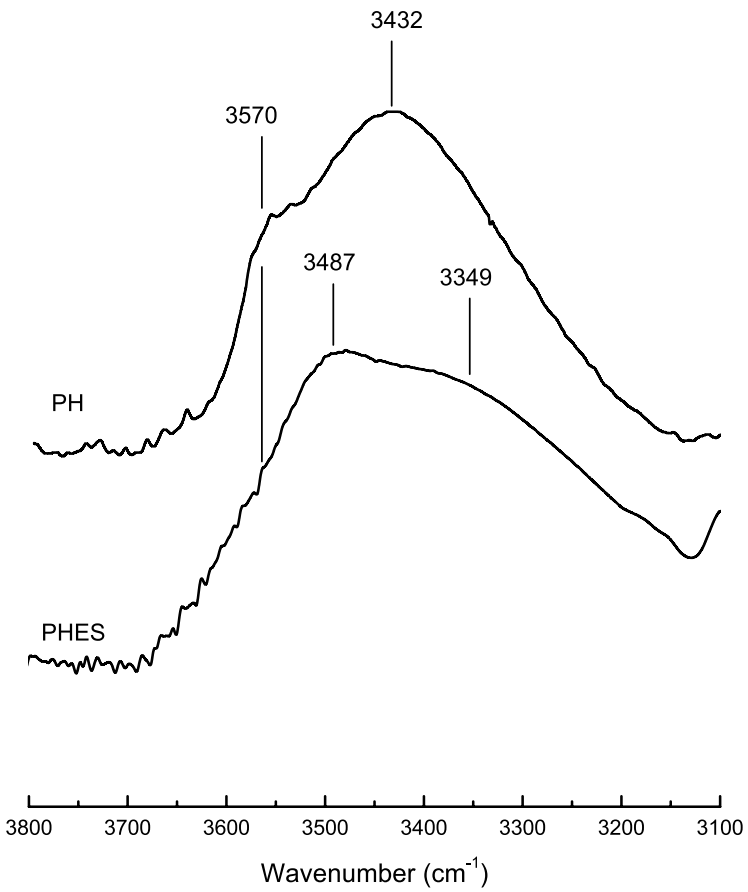

Fig. 10. Comparison of FTIR spectra in the region of 3100–3800 cm^{-1} for PHES and PH.

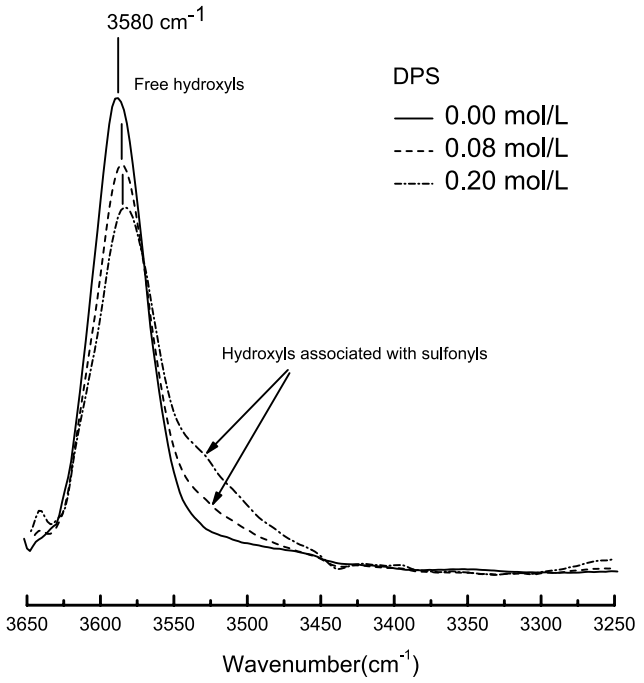

Fig. 11. FTIR difference spectra of DPS/DPP/toluene solutions with various DPS concentrations.

infrared spectra of the toluene solution of 1,3-diphenoxy-2-propanol (DPP) and 1,4-diphenyl sulfone (DPS). Fig. 11 shows the FTIR difference spectra in the hydroxyl stretching region for the mixture of DPS, DPP and toluene. For the toluene solution of DPP, only a sharp free (non-associated) hydroxyl band at 3580 cm^{-1} was displayed at the low concentration (0.02 M). Upon adding DPS to system, it is seen that the intensity (fraction) of the free hydroxyl (at 3580 cm^{-1}) of DPP decreased, whereas at the lower frequencies (ca. 3500 cm^{-1}) the ramp bands appeared, which are ascribed to sulfonyl-bonded hydroxyls and the intensity of the bands increased with increasing DPS concentration.

Compared with PH, the appearance of the hydroxyl-stretching band at the higher frequency (i.e. $\Delta\nu = 83\ cm^{-1}$) for PHES suggests that there is a formation of the weaker hydrogen bonding in PHES. The weaker hydrogen bonding interactions could be attributed to the hydroxyl groups that hydrogen-bonded with sulfonyl groups. The inference can be evidenced by the comparison of several equilibrium association constants with PHES. According to the Painter–Coleman association model [55,56], the three subscripts 2, B and S are used to denote the equilibrium constants, K_2, K_B and K_S of dimers, multimers of PHES and the self-association of PHES via hydroxyl versus sulfonyl groups, respectively. Using DPP as the model compound of structural unit of hydroxyl ether, Coleman et al. [14] and Iruin et al. [57] have separately obtained $K_2 = 12.9$ (dimensionless unit), $K_B = 21.3$ (dimensionless unit) and $K_2 = 14.4$ (dimensionless unit), $K_B = 25.6$ (dimensionless unit) for the self-association of DPP in the dilute solution of toluene, derived by infrared spectroscopic data. By means of the same method, we previously measured the K_S to be 15.6 (dimensionless unit) when we selected 1,4-diphenyl sulfone (DPS) as the model compound of sulfonyl moiety of PHES [58]. It is noted that the K_S value is quite lower than the values of $K_B = 21.3$ (dimensionless unit) and/or $K_B = 25.6$ (dimensionless unit), suggesting that the hydrogen bonding interactions between hydroxyl and sulfonyl groups are significantly weaker than the strength of hydroxyl versus hydroxyl group. This result is in a good agreement with the comparison between hydroxyl stretching vibration bands of PH and PHES as shown above.

Competitive hydrogen bonding interactions. Addition of PEO to the system could give rise to break of the self-associated hydrogen bonds of PHES and the formation of the intermolecular hydrogen bonds between PHES and PEO to some extent. The competitive interactions were investigated by means of FTIR. Fig. 12 shows the FTIR spectra of pure PHES and its blends with PEO in the region of 3000–3800 cm^{-1}. For pure PHES, the wide stretching vibration

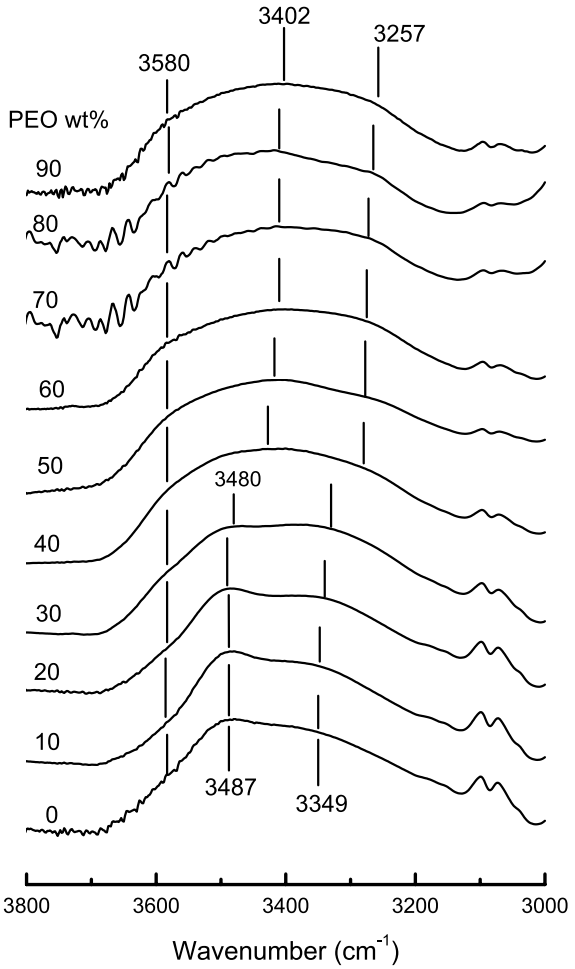

Fig. 12. FTIR Spectra of PHES/PEO blends in the region of 3000–3800 cm^{-1}. (A) PHES, (B) 70/30, (C) 50/50, (D) 30/70 and (E) 10/90.

bands of hydroxyl groups comprises of two discernible components at 3487 and 3349 cm^{-1}, respectively. The stretching vibration of free hydroxyl occurs at 3570 cm^{-1} (see Fig. 10). Upon adding PEO to the system, it was seen that the intensity of the hydroxyl stretching bands at 3487 cm^{-1} decreased with increasing PEO concentration, whereas the intensity of the hydroxyl band at 3349 cm^{-1} increased with increasing PEO content. When PEO content is up to 40 wt%, the band at 3487 cm^{-1} is indiscernible, instead, at lower frequencies (e.g. at 3402 and 3257 cm^{-1}), new hydroxyl bands appeared and the intensity of these bands increased with increasing PEO concentration. The new bands could be ascribed to the hydroxyls that are hydrogen-bonded with ether oxygen atom of PEO. It is noticed that the hydroxyl stretching bands became much more broad with the inclusion of PEO. The observation that the intensity of the bands for the hydroxyls that are hydrogen-bonded with sulfonyl groups decreased indicates that the sulfonyl-bonded hydroxyls were increasingly 'set free' upon adding PEO to system. At the same time, the appearance of the hydroxyl bands at the lower frequencies indicated that there were the formation of the stronger hydrogen bonding interactions between hydroxyls and ether oxygen atom of PEO. The results also indicated that the hydrogen bonding interactions between hydroxyls of PHES and ether oxygen atoms of PEO is much stronger than those of –OH···–OH and –OH···O=S hydrogen bonds. In terms of the frequency differences between free and H-bonded hydroxyl stretching vibration, it is judged that from weak to strong the strength of the hydrogen bonding interactions is in the following order: –OH···O=S, –OH···–OH and –OH versus ether oxygen atoms of PEO. Returning to Fig. 12, if the most-distributed hydroxyl band at ca. 3402 is used to evaluate the hydrogen bonding strength, we can obtain the value of $\Delta\nu = 168$ cm^{-1} for PHES/PEO 50/50 blend, which is significantly lower than $\Delta\nu = 270$ cm^{-1} for PH/PEO 50/50 blend [15]. The result suggests that the overall intermolecular hydrogen bonding interactions in PHES/PEO are much weaker than those in PH/PEO blends, which is in good agreement with the result of equilibrium melting point depression.

4. Conclusions

Poly(hydroxyether sulfone) (PHES) was synthesized through direct polycondensation of bisphenol S with epichlorohydrin. The structure of the polymer was characterized by means of Fourier transform infrared and nuclear magnetic resonance spectroscopy. The investigation of GPC shows that the high molecular weight polymer was obtained. FTIR investigation showed that there was the formation of the weaker intramolecular hydrogen bonding interactions via –OH···O=S than –OH···–OH in PHES. The miscibility in blends of PHES with poly(ethylene oxide) (PEO) was established on the basis of the thermal analysis results. DSC investigation showed that the PHES/PEO blends prepared by casting from *N*,*N*-dimethylformamide (DMF) possessed single, composition-dependent glass transition temperatures (T_gs); the blend system is miscible in the amorphous state at all compositions. At elevated temperatures, the PHES/PEO blends underwent phase separation. The phase behavior was investigated by optical microscope and the cloud point curve (CPC) was determined. A typical LCST behavior was observed in the moderate temperature range for this blend system. FTIR studies indicate that there is the competitive hydrogen bonding interactions upon adding PEO to the system, which was involved with –OH···O=S, –OH···–OH and hydroxyls versus ether oxygen atoms of PEO hydrogen bonds, both intramolecular and intermolecular. The break of the weaker hydrogen bonding between hydroxyls and sulfonyls within PHES and the formation of the stronger hydrogen bonding interactions between hydroxyls of PHES and ether oxygen atoms of PEO indicated that from weak to strong the strength of the hydrogen bonding interactions is in the order: –OH···O=S, –OH···–OH and –OH versus ether oxygen atoms of PEO.

Acknowledgements

The financial support from Ministry of Education, PRC under an Excellent Young Teacher Program (EYTP, Project No. 2066) was acknowledged. The authors would like to thank Natural Science Foundation of China (50390090) for the partial support.

References

[1] Olabisi O, Robeson LM, Shaw MT. Polymer–polymer miscibility. New York: Academic Press; 1979.
[2] Utracki LA. Polymer alloys and blends. Munich: Hanser Publishers; 1989.
[3] Folkes MJ, editor. Polymer blends and alloys. London: Chapman & Hall; 1993.
[4] ten Brinke G, Karasz FE. Macromolecules 1984;17:815.
[5] Sanchez IC, Balazs AC. Macromolecules 1989;22:2325.
[6] Graf JF, Coleman MM, Painter PC. J Phys Chem 1991;95:6710.
[7] Robeson LM, Hale WF, Merrian CN. Macromolecules 1981;14:1644.
[8] Iriarte M, Espi E, Etxeberria A, Valero M, Fernandez-Berridi MJ, Iruin JJ. Macromolecules 1991;24:5546.
[9] Iriarte M, Iribarren JI, Etxeberria A, Iruin JJ. Polymer 1988;30:1160.
[10] Juana Rde, Cortazar M. Macromolecules 1993;26:1170.
[11] Fernandez-Berridi MJ, Valero M, Martinez de IIarduya A, Espi E, Iruin JJ. Polymer 1993;34:38.
[12] Wu H-D, Chu PP, Ma C-CM. Polymer 1998;39:703.
[13] Martinez de IIarduya A, Iruin JJ, Fernandez-Berridi MJ. Macromolecules 1995;28:3707.
[14] Coleman MM, Yang X, Painter PC, Graf FJ. Macromolecules 1992; 25:4414.
[15] Coleman MM, Moskala EJ. Polymer 1983;24:251.
[16] Zheng S, Jungnickel B-J. J Polym Sci, Part B: Polym Phys 2000;38: 1250.
[17] Zheng S, Zhang W, Ma D. Eur Polym J 1997;33:937.

[18] Lau C, Zheng S, Zhong Z, Mi Y. Macromolecules 1998;37:291.
[19] Zheng S, Guo Q, Mi Y. J Polym Sci, Part B: Polym Phys 1998;36: 2291.
[20] Zheng S, Guo Q, Mi Y. Polymer 2003;44:867.
[21] Zheng S, Mi Y. Polymer 2003;44:1067.
[22] Zheng S, Ai S, Guo Q. J Polym Sci, Part B: Polym Phys 2003;41:466.
[23] Tanaka H, Nishi T. Phys Rev A 1989;39:783.
[24] Nishi T, Wang TT. Macromolecules 1975;8:809.
[25] Imken RL, Paul DR, Barlow JW. Polym Engng Sci 1976;16:593.
[26] Li X, Hsu SL. J Polym Sci, Part B: Polym Phys 1984;22:1331.
[27] Fox TG. Bull Am Phys Soc 1956;1:23.
[28] Gordon M, Taylor JS. J Appl Chem 1952;2:495.
[29] Belorgey G, Prud'homme RE. J Polym Sci, Polym Phys Ed 1982;20:191.
[30] Belorgey G, Aubin M, Prud'homme RE. Polymer 1982;23:1051.
[31] Aubin M, Prud'homme RE. Macromolecules 1988;21:2945.
[32] Cheung YW, Stein RS. Macromolecules 1994;27:2512.
[33] Kovacs AJ. Adv Polym Sci 1963;3:394.
[34] Pedrosa P, Pomposo JA, Calahorra E, Cortazar M. Macromolecules 1994;27:102.
[35] Braun G, Kovacs AJ. In: Prins JA, editor. Physics of non-crystalline solids. Amsterdam: North-Holland; 1965.
[36] Van Krevelen DW, Holftyzer PJ. Properties of polymer, 2nd ed. Amsterdam: Elsevier; 1980.
[37] Fernandes AC, Barlow JW, Paul DR. J Appl Polym Sci 1984;29:3381.
[38] Li Y, Stein M, Jungnickel B-J. Colloid Polym Sci 1991;269:772.
[39] Li Y, Jungnickel B-J. Polymer 1993;34:9.
[40] Jungnickel B-J. Curr Trends Polym Sci 1997;2:157.
[41] Lü H, Zheng S. Polymer 2003;44:4689.
[42] Hashimoto T, Current topics in polymer science part 6, vol. II. Munich: Hanser Publishers; 1987. p. 1.
[43] Walsh D, Singh V. Makromol Chem 1984;185:1979.
[44] Guo W, Higgins J. Polymer 1990;31:699.
[45] Dreezen G, Fang Z, Groeninckx G. Polymer 1999;40:5907.
[46] Dreezen G, Mischenko N, Koch MHJ, Reynaers H, Groeninckx G. Macromolecules 1999;32:4015.
[47] Hoffman JD, Weeks JJ. J Res Natl Bur Stand 1962;66:13.
[48] Hoffman JD, Weeks JJ. J Chem Phys 1962;37:13.
[49] Paul DR, Barlow JW, Beinstein RE, Wahrmund DC. Polym Engng Sci 1978;18:1225.
[50] Ziska JJ, Barlow JW, Paul DR. Polymer 1981;22:918.
[51] Martucelli E, Pracella M, Yue WP. Polymer 1984;25:1097.
[52] Itiarte M, Iribarren I, Etxeberria A, Iruin JJ. Polymer 1989;30:1160.
[53] Purcell KF, Drago RS. J Am Chem Soc 1968;24:251.
[54] Coleman MM, Painter PC. Appl Spectrosc Rev 1984;20:225.
[55] Coleman MM, Painter PC. Prog Polym Sci 1995;20:1.
[56] Coleman MM, Graf JF, Painter PC. Specific interactions and the miscibility of polymer blends. Lancaster, PA: Technomic Publishing; 1991.
[57] Espi E, Alberdi M, Fernandez-Berridi MJ, Iruin JJ. Polymer 1994;35: 3712.
[58] Lü H, Zheng S, Zhang B. Macromol Chem Phys 2004; in press.